Analytical theory of hysteresis in ion channels: Two-state model

M. A. Pustovoit
St. Petersburg Nuclear Physics Institute, Gatchina 188300, Russia

A. M. Berezhkovskii
Mathematical and Statistical Computing Laboratory, Division of Computational Bioscience, Center for Information Technology, National Institutes of Health, Bethesda, Maryland 20892

S. M. Bezrukov[a)]
Laboratory of Physical and Structural Biology, National Institute of Child Health and Human Development, National Institutes of Health, Bethesda, Maryland 20892

(Received 30 June 2006; accepted 27 September 2006; published online 20 November 2006)

Channel-forming proteins in a lipid bilayer of a biological membrane usually respond to variation of external voltage by changing their conformations. Periodic voltages with frequency comparable with the inverse relaxation time of the protein produce hysteresis in the occupancies of the protein conformations. If the channel conductance changes when the protein jumps between these conformations, hysteresis in occupancies is observed as hysteresis in ion current through the channel. We develop an analytical theory of this phenomenon assuming that the channel conformational dynamics can be described in terms of a two-state model. The theory describes transient behavior of the channel after the periodic voltage is switched on as well as the shape and area of the hysteretic loop as functions of the frequency and amplitude of the applied voltage. The area vanishes as the voltage period T tends to zero and infinity. Asymptotic behaviors of the loop area A in the high- and low-frequency regimes, respectively, are $A \sim T$ and $A \sim T^{-1}$.
 [DOI: 10.1063/1.2364898]

I. INTRODUCTION

This paper deals with hysteresis in voltage-gated ion channels. A distinctive feature of such a channel is high sensitivity of its conformational equilibrium to the transmembrane voltage. Because of significantly different conductances of different conformations of the channel-forming protein molecule, this results in a strong nonlinearity of the channel stationary current-voltage characteristics.[1] However, equilibration of the channel-forming protein may occur very slowly. When the period of the applied transmembrane voltage is comparable with the protein equilibration time, the ion current through the channel depends on prehistory, and one meets standard conditions under which hysteresis is observed. In the present paper we develop an analytical theory of hysteresis for a two-state model of the protein voltage gating. Although the model is greatly simplified, we believe that our results will be used as a benchmark for studying hysteresis in voltage-gated ion channels.

Hysteresis is ubiquitous both in nature and in man-made devices. In voltage-gated channels, it has been studied experimentally for more than two decades. One can find recent discussions of such studies,[2–7] which also include the question of physiological significance of the hysteretic response. For example, it was proposed that channel hysteresis plays a beneficial role in maintaining regular firing of a neuron pacemaker.[6] Computer simulations of hysteresis are used to discriminate between different kinetic models of the channel gating.[2,6] However, to the best of our knowledge, no analytical studies of hysteresis in voltage-gated channels have been performed even for the simplest case of a two-state model. The goal of the present study is to fill this gap.

A function frequently used when discussing hysteresis is the hysteresis loop area. The loop area depends on the frequency and amplitude of the applied periodic voltage as well as on the protocol of the voltage change. In the absence of static hysteresis, the loop area vanishes in two limiting cases of very slow and very fast voltage change. When the voltage varies sufficiently slowly, the protein molecule has enough time to adjust its conformational distribution to the instantaneous value of the voltage. As a consequence, the ion current through the channel is independent of the prehistory and hence there is no hysteresis. In the opposite limiting case, when the period of the voltage change is much shorter than the characteristic protein relaxation time, the protein molecule cannot follow fast variations of the voltage and sees only its average value. As a consequence, the current through the channel becomes again independent of the prehistory, and the hysteresis loop collapses to a single line. Thus, the loop area first monotonically grows with the frequency of voltage change, reaches a maximum, and then goes to zero, as the frequency tends to infinity.

In the present paper we develop a theory of hysteresis in voltage-gated ion channels in the framework of a two-state model of gating, which is discussed in the next section. In Sec. III we derive transient behavior of the channel after the periodic external voltage is switched on. An expression for the hysteresis loop area is derived in Sec. IV. In this section we also show that in one special case this expression leads to

[a)]Electronic mail: bezrukos@mail.nih.gov

an explicit formula for the loop area. In the general case we use the expression to study the dependence of the loop area on the voltage period and amplitude including its asymptotic behavior at low and high frequencies. We compare our results with those obtained in other studies of hysteresis in Sec. V.

II. THE MODEL

Consider a membrane containing N channels each of which can be in one of the two conformational states of differing conductances. Electrolyte solutions on both sides of the membrane are identical. When constant voltage V is applied, ion current through the membrane is given by

$$I = N[P_1 g_1 + (1 - P_1) g_2]V, \tag{2.1}$$

where g_i is conductance of an individual channel in state i, $i=1,2$, and P_1 is the equilibrium probability of finding the channel in state 1, which is a function of V, $P_1=P_1(V)$. In principle, the conductances g_i may be voltage dependent, but we do not consider this case here. The current-voltage characteristics of the membrane are highly nonlinear when the conductances g_1 and g_2 are substantially different, and the probability $P_1(V)$ significantly varies over the range of voltages used in experiment.

We will assume that transitions between the two states are Markovian and can be described by the kinetic scheme

$$1 \underset{k_2}{\overset{k_1}{\rightleftarrows}} 2 \tag{2.2}$$

with voltage-dependent transition rates k_1 and k_2 given by

$$k_1 = k_1^{(0)} \exp(-\alpha_1 V), \quad k_2 = k_2^{(0)} \exp(\alpha_2 V), \tag{2.3}$$

where $k_i^{(0)}$, $i=1,2$, are the rates in the absence of the external voltage and positive factors α_i are inversely proportional to the absolute temperature. The equilibrium fractional population of state 1 is

$$P_1(V) = k_2 \tau, \tag{2.4}$$

where τ is the equilibration time,

$$\tau = k^{-1}, \quad k = k_1 + k_2. \tag{2.5}$$

The kinetic scheme in Eq. (2.2) with the rate constants in Eq. (2.3) implies that the two states correspond to two deep wells of the double-well potential surface. It is assumed that the applied voltage can be sufficiently high to significantly change equilibrium occupancies of the two wells by varying the well energies. At the same time the voltage is not high enough to destroy the double-well structure of the potential surface, so that the wells are separated by a high barrier over the entire range of voltages used in experiment. Description of voltage gating in terms of the kinetic scheme in Eq. (2.2), to the best of our knowledge, for the first time was proposed by Mueller and Rudin[8] and demonstrated for individual channels by Ehrenstein *et al.*[9] Double-well models of voltage-gated channels of this type have recently been studied in the framework of Kramers theory of activated rate processes by Sigg *et al.*[10] and Bezanilla.[11]

When the applied voltage is a function of time, the rate coefficients in Eq. (2.3) are time dependent and the probability $P_1(t)$ of finding the channel in state 1 at time t can be found by solving the rate equation

$$\frac{dP_1(t)}{dt} = -k_1(t)P_1(t) + k_2(t)[1 - P_1(t)]$$
$$= k_2(t) - k(t)P_1(t), \tag{2.6}$$

where $k(t)=k_1(t)+k_2(t)$. The solution is

$$P_1(t) = P_1(t_0)e^{-\int_{t_0}^{t} k(t_1)dt_1} + \int_{t_0}^{t} k_2(t_1)e^{-\int_{t_1}^{t} k(t_2)dt_2}dt_1. \tag{2.7}$$

The probability in Eq. (2.7) is used below both when analyzing the transient behavior of the channel after the periodic voltage has been switched on (Sec. III) and when deriving the expression for the hysteresis loop area in Sec. IV.

Concluding this section we note that our model of voltage gating is greatly simplified, at least, in two respects.

- Electric measurements tell us only about conductance of the channel. One can easily imagine that many different conformations of the channel-forming protein may lead to virtually the same channel conductance. As a consequence, transitions between the states of different conductance, in general, cannot be described by a simple Markovian model in Eq. (2.2).[12,13]
- Dynamics of a channel-forming protein inserted into a membrane is described in terms of transitions among local minima of a very highly dimensional energy landscape. Reduction to the Markovian two-state model in Eq. (2.2) implies dramatic decrease of the dimensionality that, in general, is highly improbable.

For example, one can easily imagine a non-Markovian generalization of the two-state model in Eq. (2.2). Recent analyses[14,15] of gating of a single potassium BK channel provide evidence for the non-Markovian character of the channel dynamics.

With all this in mind, we note that the two-state model in Eq. (2.2) is the simplest model that still captures the most essential properties of the voltage-gated channels.[1,4,6–9] It is surprising therefore that this model has not been studied analytically with respect to its hysteretic properties yet.

III. TRANSIENT BEHAVIOR

Suppose that periodic voltage of period T is switched on at $t=0$. The current through the channel at time t is given by [cf. Eq. (2.1)]

$$I(t) = N[g_2 + (g_1 - g_2)P_1(t)]V(t). \tag{3.1}$$

Here $V(t)$ is the time-dependent external voltage of the form $V(t)=H(t)V_T(t)$, where $H(t)$ is the Heaviside step function and $V_T(t)$ is a periodic function of t, $V_T(t+T)=V_T(t)$. As $t\to\infty$, both $P_1(t)$ and the current $I(t)$ become periodic, $P_1(t+T)=P_1(t)$ and $I(t+T)=I(t)$. In this section we study transient behavior of $P_1(t)$. In what follows we consider only the probability of finding the channel in state 1. Therefore,

we omit the subscript in the notation of this probability, i.e., $P_1(t) \to P(t)$ hereafter.

Using the solution in Eq. (2.7) we can write $P(t)$ for $nT < t < (n+1)T$, $n=0,1,\ldots$, which we denote $P(t|n)$ as

$$P(t|n) = P(nT)\exp\left[-\int_{nT}^{t} k(t_1)dt_1\right] + \int_{nT}^{t} k_2(t_2)\exp\left[-\int_{t_2}^{t} k(t_1)dt_1\right]dt_2. \tag{3.2}$$

In addition, using Eq. (2.7) one can write a recursion formula connecting the probabilities $P(nT)$ and $P((n+1)T)$:

$$P((n+1)T) = \gamma P(nT) + a_0, \tag{3.3}$$

where γ and a_0 are given by

$$\gamma = \exp\left[-\int_0^T k(t)dt\right] \tag{3.4}$$

and

$$a_0 = \int_0^T k_2(t_2)\exp\left[-\int_{t_2}^{T} k(t_1)dt_1\right]dt_2. \tag{3.5}$$

The recursion formula in Eq. (3.3) allows us to express $P(nT)$ in terms of $P(0)$ which is the equilibrium probability of finding the channel in state 1 in the absence of external voltage, $P(0)=k_2^0/(k_1^0+k_2^0)$. Eventually we obtain

$$P(nT) = \gamma^n \frac{k_2^{(0)}}{k_1^{(0)}+k_2^{(0)}} + \frac{1-\gamma^n}{1-\gamma}a_0. \tag{3.6}$$

Expressions in Eqs. (3.2) and (3.6) give the probability $P(t)$ at any t. As $n \to \infty$ the probability $P(nT)$ approaches its asymptotic value,

$$\lim_{n\to\infty} P(nT) = \frac{a_0}{1-\gamma}. \tag{3.7}$$

Substituting this into Eq. (3.2) we find the asymptotic long-time behavior of the probability $P(t)$, which will be denoted by $P_\infty(t)$,

$$P_\infty(t) = \lim_{n\to\infty} P(t|n) = \frac{a(t)}{1-\gamma}, \tag{3.8}$$

where function $a(t)$ is given by

$$a(t) = \int_t^{t+T} k_2(t_2)\exp\left[-\int_{t_2}^{t+T} k(t_1)dt_1\right]dt_2. \tag{3.9}$$

One can see that $a(0)=a_0$. Function $a(t)$ is periodic, $a(t+T)=a(t)$. As a consequence, $P_\infty(t)$ is also periodic, $P_\infty(t+T)=P_\infty(t)$. Transient behavior of $P(t)$ from $P(0)$ to $P_\infty(t)$ is illustrated in Fig. 1.

The expression for $P_\infty(t)$ in Eq. (3.8) is used in the next section to study the area of the hysteresis loop. Expressions in Eqs. (3.8) and (3.9) show that $P_\infty(t)$ is prehistory dependent. This dependence disappears in the limiting cases of very slow and very fast variation of the voltage (Fig. 2). In these limiting cases $P_\infty(t)$ takes the form

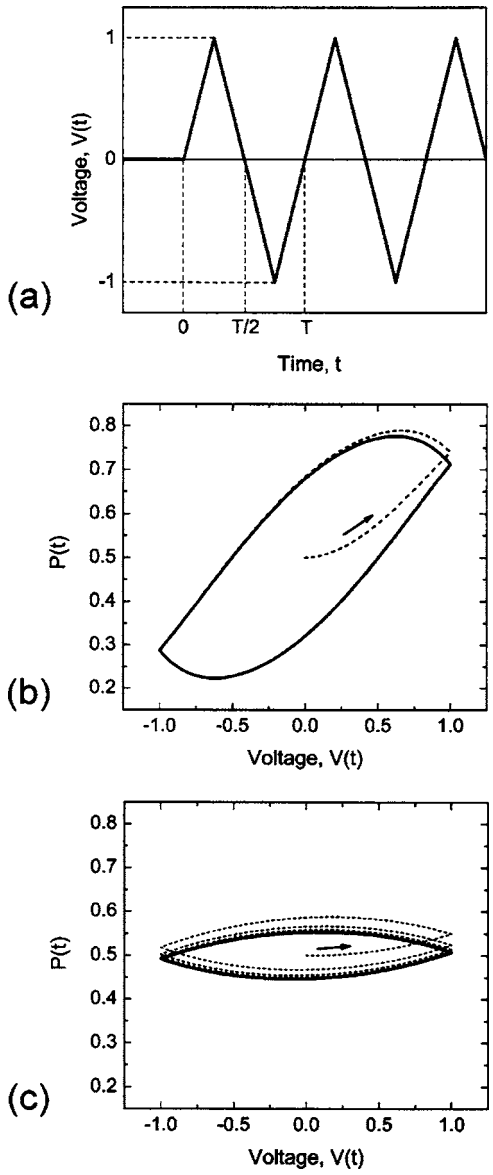

FIG. 1. Transition of the probability $P(t)$ from its equilibrium value in the absence of voltage, $P(0)=0.5$, to its long-time asymptotic form $P_\infty(t)$ given in Eqs. (3.8) and (3.9). Symmetric periodic external voltage of unit amplitude is switched on at $t=0$. The voltage protocol is shown in panel (a). It is taken that $k_i^{(0)}=1$, $\alpha_i=1$. Transient behavior (dashed curves) was found using Eqs. (3.2) and (3.4)–(3.6) for $T=3.16$ [panel (b)] and $T=0.40$ [panel (c)]. Solid curves give $P_\infty(t)$. The shorter is the period, the more cycles it takes for the system to reach $P_\infty(t)$ and the smaller the deviations of $P(t)$ from its equilibrium value $P(0)=0.5$ are.

$$P_\infty(t) = \frac{k_2(t)}{k(t)} \quad \text{for slow } V(t) \tag{3.10}$$

and

$$P_\infty(t) = \frac{\langle k_2\rangle}{\langle k\rangle} \quad \text{for fast } V(t), \tag{3.11}$$

where the angular brackets denote averaging over the period of a periodic function $f(t)$,

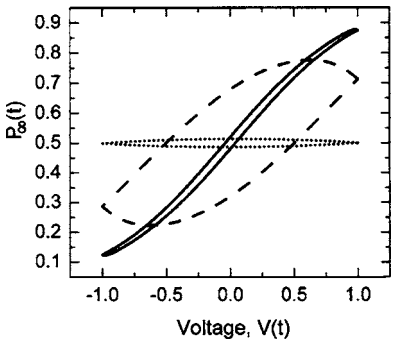

FIG. 2. The hysteresis loops $P_\infty(t)$ vs voltage $V(t)$ corresponding to the periodic voltage that changes linearly in time between 1 and −1 for three values of the period: $T=50.12$ (solid curve), 3.16 (dashed curve), and 0.10 (dotted curve). It is taken that $k_i^{(0)}=1$, $\alpha_i=1$. One can see that the loop area goes to zero for both very slow and very fast variations of the applied voltage.

$$\langle f\rangle = \frac{1}{T}\int_0^T f(t)dt. \tag{3.12}$$

Thus, in the latter limiting case, $P_\infty(t)$ is independent of time. As soon as $P_\infty(t)$ becomes independent of the prehistory, the loop area vanishes since the loop collapses to a single line (Fig. 2).

IV. THE LOOP AREA

In this section we analyze the loop area assuming that

$$V_T(t) = \Delta V \varphi_T(t), \tag{4.1}$$

where ΔV is the amplitude of the external voltage, $\Delta V>0$, and $\varphi_T(t)$ is a periodic function of time of period T, $\varphi_T(t+T)=\varphi_T(t)$, which varies between unity and minus unity. It will be assumed that $\varphi_T(t)$ reaches its maximum and minimum values at $t=0$ and $t=\pm T/2$, respectively, i.e., $\varphi_T(0)=1$ and $\varphi_T(\pm T/2)=-1$. In addition, we assume that $\varphi_T(t)$ is symmetric, i.e., $\varphi_T(t)=\varphi_T(-t)$ and $\varphi_T(t)=-\varphi_T(T/2-t)$, the latter holds for $0\leqslant t\leqslant T/4$. As an example, in Fig. 3 we show

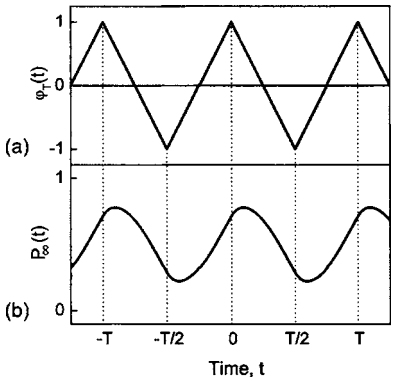

FIG. 3. Time course of probability $P_\infty(t)$ [panel (b)] corresponding to the protocol in Eq. (4.1) with $\Delta V=1$ and $\varphi_T(t)$ given in Eq. (4.2) [panel (a)] for $T=3.16$. It is taken that $k_i^{(0)}=1$, $\alpha_i=1$. The shape of the hysteretic loop is shown in Fig. 2 by the dashed curve.

$$\varphi_T(t) = 1 - \frac{4|t|}{T}, \quad -\frac{T}{2}\leqslant t\leqslant \frac{T}{2} \tag{4.2}$$

and the corresponding $P_\infty(t)$.

The hysteresis loop area for the probability of finding the channel in state 1 is given by

$$A(T) = \int_0^{T/2} P_\infty(t)|\dot V_T(t)|dt - \int_{-T/2}^0 P_\infty(t)|\dot V_T(t)|dt, \tag{4.3}$$

where we have used the dot above $V_T(t)$ as a notation for the derivative with respect to time. Using $V_T(t)$ in Eq. (4.1) we can write the loop area $A(T)$ as

$$A(T) = 4\Delta V \tilde A(T), \tag{4.4}$$

where the dimensionless loop area $\tilde A(T)$ is defined by

$$\tilde A(T) = \frac{1}{4}\int_0^{T/2} [P_\infty(t) - P_\infty(-t)]|\dot\varphi_T(t)|dt. \tag{4.5}$$

One can see that $A(T)=\tilde A(T)=0$ when $P_\infty(t)$ is independent of the prehistory, as it must be. Our further analysis is mainly focused on the dimensionless loop area $\tilde A(T)$.

Expressions in Eqs. (3.8) and (4.5) are one of the main results of the present paper. They allow one to find the loop area at arbitrary T and ΔV. We demonstrate how it works for the protocol in Eq. (4.2) in Sec. IV D. Before that we discuss limiting behavior of $\tilde A(T)$ in the low-and high-frequency regimes in Secs. IV B and IV C and give the explicit solution for the entire frequency range by means of the perturbation theory in the following subsection.

A. Explicit solution for $\tilde A(T)$ by perturbation theory

In this subsection we assume that ΔV is small in the sense that $\alpha_i\Delta V\ll 1$, $i=1,2$. Then the rate constants $k_i(t)$ are approximately

$$k_1(t) \simeq k_1^{(0)} - \Delta k_1\varphi_T(t), \quad k_2(t)\simeq k_2^{(0)} + \Delta k_2\varphi_T(t), \tag{4.6}$$

where $\Delta k_i=\alpha_i\Delta V k_i^{(0)}$ are small compared to $k_i^{(0)}$, $\Delta k_i\ll k_i^{(0)}$. In addition, we assume that $\Delta k_1=\Delta k_2$. Respectively, for $k(t)=k_1(t)+k_2(t)$, this leads to

$$k(t)\simeq k_1^{(0)} + k_2^{(0)} = k_0. \tag{4.7}$$

We use the above approximations to write $a(t)$ defined in Eq. (3.9) as

$$a(t)\simeq \frac{1}{k_0}[k_2^{(0)}(1-\gamma) + \Delta k_2 f(t)], \tag{4.8}$$

where the function $f(t)$ is defined by

$$f(t) = k_0\exp[-k_0(t+T)]\int_t^{t+T}\varphi_T(t')\exp(k_0t')dt', \tag{4.9}$$

and γ defined in Eq. (3.4) is approximately

$$\gamma \simeq \exp(-k_0 T). \tag{4.10}$$

Eventually we can write $P_\infty(t)$ in Eq. (3.8) as

$$P_\infty(t) \simeq P_{\rm eq}^{(0)}\left[1+\frac{\alpha_2 \Delta V}{1-\gamma} f(t)\right], \tag{4.11}$$

where $P_{\rm eq}^{(0)}=k_2^{(0)}/k_0$ is the equilibrium probability of finding the channel in state 1 in the absence of external voltage, i.e., $P_1(V)$ in Eq. (2.4) at $V=0$. Equation (4.11) provides the perturbation theory solution for $P_\infty(t)$. Substituting this $P_\infty(t)$ into Eq. (4.5), we obtain the perturbation theory result for the dimensionless loop area,

$$\tilde{A}(T)=\frac{\alpha_2 \Delta V P_{\rm eq}^{(0)}}{4(1-\gamma)}\int_0^{T/2}[f(t)-f(-t)]|\dot{\varphi}_T(t)|dt. \tag{4.12}$$

Now we assume that $\varphi_T(t)$ is given by Eq. (4.2). For this protocol $f(t)$ and, hence, $P_\infty(t)$ can be found explicitly. The result is

$$f(t)=(1-\gamma)\left[1+\frac{4}{k_0 T} f_1(t)\right], \tag{4.13}$$

where function $f_1(t)$ is given by

$$f_1(t)=\begin{cases} 1-k_0 t-\dfrac{2\exp(-k_0 t)}{1+\exp(-k_0 T/2)}, & 0\leqslant t\leqslant \dfrac{T}{2} \\ -1+k_0 t+\dfrac{2\exp(-k_0 t)}{1+\exp(k_0 T/2)}, & -\dfrac{T}{2}\leqslant t\leqslant 0. \end{cases} \tag{4.14}$$

Eventually we obtain

$$\begin{aligned}\tilde{A}(T)&=\frac{4\alpha_2 \Delta V P_{\rm eq}^{(0)}}{k_0 T^2}\int_0^{T/2}[f_1(t)-f_1(-t)]dt \\ &=\alpha_2 \Delta V P_{\rm eq}^{(0)} F\left(\frac{k_0 T}{4}\right),\end{aligned} \tag{4.15}$$

where function $F(x)$ is

$$F(x)=\frac{1}{x}\left(1-\frac{\tanh x}{x}\right). \tag{4.16}$$

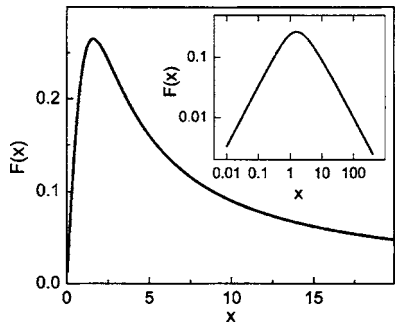

FIG. 4. Plot of $F(x)$ in Eq. (4.16). The inset shows the same plot in double logarithmic coordinates.

$F(x)$ is a bell-shaped function. Its plot is shown in Fig. 4.

As follows from Eqs. (4.15) and (4.16), the loop area vanishes as T goes to zero and infinity. Asymptotic behavior of $\tilde{A}(T)$ in these two limiting cases is given by

$$\tilde{A}(T)=\alpha_2 \Delta V P_{\rm eq}^{(0)}\begin{cases}\dfrac{k_0 T}{12}, & k_0 T \ll 1 \\ \dfrac{4}{k_0 T}, & k_0 T \gg 1. \end{cases} \tag{4.17}$$

We will see that the asymptotic T dependences of the loop area predicted by the perturbation theory hold also for arbitrary ΔV and for the voltage protocol $\varphi_T(t)$ which is not necessarily the one in Eq. (4.2).

B. Low-frequency regime ($T\to\infty$)

In the low-frequency regime, when $T\to\infty$, γ defined in Eq. (3.4) vanishes and $P_\infty(t)$ in Eq. (3.8) takes the form

$$P_\infty(t)=a(t)=\int_0^T k_2(t-t_2)\exp\left[-\int_0^{t_2} k(t-t_1)dt_1\right]dt_2. \tag{4.18}$$

When evaluating $P_\infty(t)$ in this regime, it is justified to use the following approximations:

$$k_2(t-t_2)\simeq k_2(t)-t_2\dot{k}_2(t), \quad k(t-t_1)\simeq k(t)-t_1\dot{k}(t), \tag{4.19}$$

and

$$\exp\left[-\int_0^{t_2} k(t-t_1)dt_1\right]\simeq\left(1+\frac{1}{2}\dot{k}(t)t_2^2\right)\exp[-k(t)t_2], \tag{4.20}$$

which exploit the fact that the rate coefficients are slowly varying functions of time. Neglecting the term proportional to the product $\dot{k}(t)\dot{k}_2(t)$, after some manipulations we eventually obtain

$$P_\infty(t)\simeq P_{\rm eq}(t)-\frac{1}{k(t)}\dot{P}_{\rm eq}(t), \tag{4.21}$$

where $P_{\rm eq}(t)=k_2(t)/k(t)$.

For our further analysis it is convenient to rewrite Eq. (4.21) as

$$P_\infty(t) \simeq \frac{k_2(t)}{k(t)} - \frac{k_1(t)\dot{k}_2(t) - k_2(t)\dot{k}_1(t)}{[k(t)]^3}. \tag{4.22}$$

Next we use the relations $k_1(t)=k_1^{(0)}\exp[-\alpha_1\Delta V\varphi_T(t)]$ and $k_2(t)=k_2^{(0)}\exp[\alpha_2\Delta V\varphi_T(t)]$ to write $P_\infty(t)$ in the form

$$P_\infty(t) \simeq \frac{k_2(t)}{k(t)} - (\alpha_1+\alpha_2)\Delta V\dot{\varphi}_T(t)\frac{k_1(t)k_2(t)}{[k(t)]^3}. \tag{4.23}$$

Substituting this into Eq. (4.5) and using the fact that for symmetric $\varphi_T(t)$ the derivatives satisfy $\dot{\varphi}_T(t)=-\dot{\varphi}_T(-t)$, we arrive at

$$\tilde{A}(T) = -2(\alpha_1+\alpha_2)\Delta V\int_0^{T/2}\frac{k_1(t)k_2(t)}{[k(t)]^3}\dot{\varphi}_T(t)|\dot{\varphi}_T(t)|dt. \tag{4.24}$$

Function $\varphi_T(t)$ and, hence, the rate coefficients $k_1(t)$, $k_2(t)$, and $k(t)$ are functions of the dimensionless argument t/T. Therefore, as $T\to\infty$, the loop area tends to zero as $1/T$.

For the protocol in Eq. (4.2) the loop area, Eq. (4.24), is

$$\tilde{A}(T) = \frac{2}{T}(\alpha_1+\alpha_2)k_1^{(0)}k_2^{(0)} \times\int_{-\Delta V}^{\Delta V}\frac{\exp[(\alpha_2-\alpha_1)\xi]d\xi}{[k_1^{(0)}\exp(-\alpha_1\xi)+k_2^{(0)}\exp(\alpha_2\xi)]^3}. \tag{4.25}$$

When $\Delta V\to 0$ the integral simplifies and $\tilde{A}(T)$ takes the form

$$\tilde{A}(T) = \frac{4(\alpha_1+\alpha_2)\Delta V k_1^{(0)}k_2^{(0)}}{Tk_0^3}. \tag{4.26}$$

One can check that for $\Delta k_1=\Delta k_2$, this is identical to the perturbation theory result in Eq. (4.17) with $k_0T\gg 1$, as it must be. The integral in Eq. (4.25) is a monotonic function of ΔV. As $\Delta V\to\infty$ the integral tends to its finite upper limit, and $\tilde{A}(T)$ takes the form

$$\tilde{A}(T) = \frac{2}{T}(\alpha_1+\alpha_2)k_1^{(0)}k_2^{(0)} \times\int_{-\infty}^{\infty}\frac{\exp[(\alpha_2-\alpha_1)\xi]d\xi}{[k_1^{(0)}\exp(-\alpha_1\xi)+k_2^{(0)}\exp(\alpha_2\xi)]^3}. \tag{4.27}$$

C. High-frequency regime ($T\to 0$)

In the high-frequency regime, when $T\to 0$, γ in Eq. (3.4) is approximately $\gamma=1-T\langle k\rangle$. As a result, Eq. (3.8) takes the form

$$P_\infty(t) = \frac{1}{T\langle k\rangle}\int_t^{t+T}k_2(t_2)dt_2\exp\left[-\int_{t_2}^{t+T}k(t_1)dt_1\right]. \tag{4.28}$$

Using the approximation

$$\exp\left[-\int_{t_2}^{t+T}k(t_1)dt_1\right] \simeq 1-\int_{t_2}^{t+T}k(t_1)dt_1, \tag{4.29}$$

we can write $P_\infty(t)$ in Eq. (4.28) as

$$P_\infty(t) = \frac{\langle k_2\rangle}{\langle k\rangle} - \frac{1}{T\langle k\rangle}\int_t^{t+T}k(t_1)dt_1\int_t^{t_1}k(t_2)dt_2. \tag{4.30}$$

Since $k(t)=k_1(t)+k_2(t)$ and

$$\int_t^{t+T}k_2(t_1)dt_1\int_t^{t_1}k_2(t_2)dt_2 = \frac{1}{2}T^2\langle k_2\rangle^2, \tag{4.31}$$

the expression in Eq. (4.30) reduces to

$$P_\infty(t) = \frac{\langle k_2\rangle}{\langle k\rangle} - \frac{T\langle k_2\rangle^2}{2\langle k\rangle} - \frac{1}{T\langle k\rangle}\int_t^{t+T}k_1(t_1)dt_1\int_t^{t_1}k_2(t_2)dt_2. \tag{4.32}$$

The double integral above is proportional to T^2. Using the product $\langle k_1\rangle\langle k_2\rangle$ as a scale for the integrand, we eventually can write $P_\infty(t)$ as

$$P_\infty(t) = \frac{\langle k_2\rangle}{\langle k\rangle}\left\{1-\frac{T}{4}[2\langle k_2\rangle+\langle k_1\rangle G(t)]\right\}, \tag{4.33}$$

where $G(t)$ is a dimensionless function of the order of unity defined by

$$G(t) = \frac{4}{T^2\langle k_1\rangle\langle k_2\rangle}\int_t^{t+T}k_1(t_1)dt_1\int_t^{t_1}k_2(t_2)dt_2. \tag{4.34}$$

Substituting $P_\infty(t)$ in Eq. (4.33) into Eq. (4.5), we arrive at

$$\tilde{A}(T) = \frac{T\langle k_1\rangle\langle k_2\rangle}{16\langle k\rangle}\int_0^{T/2}[G(-t)-G(t)]|\dot{\varphi}_T(t)|dt. \tag{4.35}$$

Since the integral in Eq. (4.35) is independent of T, the loop area in the high-frequency regime is proportional to T and vanishes as $T\to 0$, as has been mentioned earlier.

For the protocol in Eq. (4.2), the averaged rate coefficients are given by

$$\langle k_i\rangle = \frac{1}{T}\int_0^T k_i(t)dt = \frac{k_i^{(0)}}{\Delta_i}\sinh(\Delta_i), \tag{4.36}$$

where $\Delta_i=\alpha_i\Delta V$, $i=1,2$. Straightforward integrations allow one to find function $G(t)$:

$$G(t) = \begin{cases} \dfrac{\exp[-\Delta_1\varphi_T(t)]-\exp[-\Delta_1]}{\sinh\Delta_1} + \dfrac{\exp[\Delta_2\varphi_T(t)]-\exp[-\Delta_2]}{\sinh\Delta_2}, & 0\le t\le\dfrac{T}{2} \\ \dfrac{\exp[\Delta_1]-\exp[-\Delta_1\varphi_T(t)]}{\sinh\Delta_1} + \dfrac{\exp[\Delta_2]-\exp[\Delta_2\varphi_T(t)]}{\sinh\Delta_2}, & -\dfrac{T}{2}\le t\le 0. \end{cases} \tag{4.37}$$

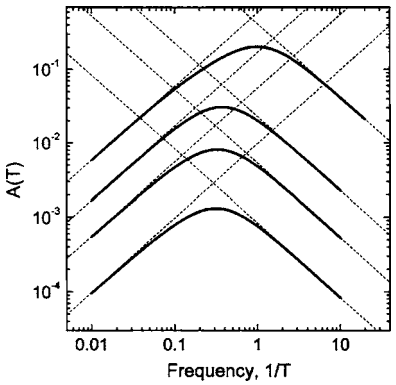

FIG. 5. The loop area $A(T)$ computed using Eq. (4.41) with $P_\infty(t)$ in Eq. (3.8) (solid curves) as a function of the frequency T^{-1} for four values of the voltage amplitude, $\Delta V=0.2$, 0.5, 1.0, 3.0, from bottom to top. It is taken that $k_i^{(0)}=1$, $\alpha_i=1$. Dashed straight lines are drawn using asymptotic behavior of $\tilde{A}(T)$ in the low-and high-frequency regimes given in Eqs. (4.25) and (4.38), respectively.

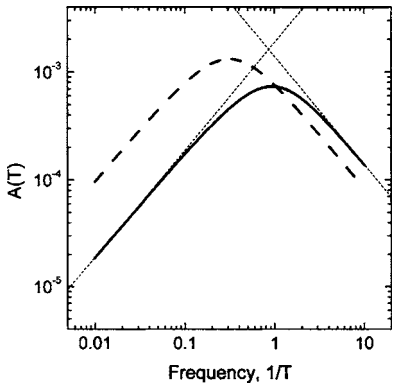

FIG. 6. The loop area $A(T)$ for an asymmetric channel (solid curve) as a function of frequency. The loop area was computed using Eq. (4.41) with $P_\infty(t)$ in Eq. (3.8) taking $k_1^{(0)}=1$, $k_2^{(0)}=5$, $\alpha_i=1$, and $\Delta V=0.2$. Dashed straight lines show low- and high-frequency behaviors of $A(T)$ obtained by using $\tilde{A}(T)$ given in Eqs. (4.25) and (4.38), respectively. For the purpose of comparison, by the dashed curve we show $A(T)$ for the symmetric channel (the bottom curve in Fig. 5).

Using this $G(t)$ one can find $\tilde{A}(T)$ in the high-frequency regime. The result is

$$\tilde{A}(T)=\frac{T\langle k_1\rangle\langle k_2\rangle}{4\langle k\rangle}\left[\frac{1}{\tanh\Delta_1}-\frac{1}{\Delta_1}+\frac{1}{\tanh\Delta_2}-\frac{1}{\Delta_2}\right]. \tag{4.38}$$

When ΔV and, hence, Δ_i tend to zero, the loop area takes the asymptotic form

$$\tilde{A}(T)=\frac{Tk_1^{(0)}k_2^{(0)}}{12k_0}(\alpha_1+\alpha_2)\Delta V, \tag{4.39}$$

which reduces to the perturbation theory result in Eq. (4.17) for $k_0T\ll 1$ when $\Delta k_1=\Delta k_2$, as it must be. In the opposite limiting case, i.e., when ΔV, $\Delta_i\to\infty$, Eq. (4.38)reduces to

$$\tilde{A}(T)=\frac{T\langle k_1\rangle\langle k_2\rangle}{2\langle k\rangle}$$

$$\simeq\frac{Tk_1^{(0)}k_2^{(0)}\exp[(\alpha_1+\alpha_2)\Delta V]}{4\Delta V[\alpha_2k_1^{(0)}\exp(\alpha_1\Delta V)+\alpha_1k_2^{(0)}\exp(\alpha_2\Delta V)]}. \tag{4.40}$$

D. Numerical results

In this section the general formula for $A(T)$ in Eq. (4.4) is used to compute the loop area over the entire range of frequencies. This is done for the protocol $V_T(t)$ in Eq. (4.1) with $\varphi_T(t)$ given in Eq. (4.2). For this special case Eq. (4.4) takes the form

$$A(T)=\Delta V\tilde{A}(T),\quad \tilde{A}(T)=\frac{1}{T}\int_0^{T/2}[P_\infty(t)-P_\infty(-t)]dt. \tag{4.41}$$

In Fig. 5 we show the computed frequency dependences of $A(T)$ for a symmetric channel with $k_i^{(0)}=1$ and $\alpha_i=1$. The dependences were computed for four values of the voltage amplitude, $\Delta V=0.2,0.5,1.0,3.0$. The computed dependences are compared with the asymptotic behavior of $A(T)$ obtained by using corresponding results for $\tilde{A}(T)$ given in Eqs. (4.25) and (4.38) for low and high frequencies, respectively. One can see excellent agreement between the theoretical predictions and computed $A(T)$ in the two limiting cases.

For illustrative purposes we also computed the frequency dependence of $A(T)$ for an asymmetric channel. This was done using Eq. (4.41) with $P_\infty(t)$ in Eq. (3.8) for a channel with $k_1^{(0)}=1$ and $k_2^{(0)}=5$ assuming that $\alpha_i=1$. The voltage amplitude was taken to be equal to 0.2. The results are given in Fig. 6 where we also show the theoretically predicted asymptotic dependences at low and high frequencies as well as the loop area for the symmetric channel with $k_1^{(0)}=k_2^{(0)}=1$ and $\alpha_i=1$. One can see that excellent agreement between the theoretical predictions and computed dependences holds for both symmetric and asymmetric channels.

V. CONCLUDING REMARKS

In the present paper we have analyzed hysteresis in ion channels on the basis of the two-state model shown in Eq. (2.2). We considered both the hysteresis loop area and transition behavior of the channel after periodic external voltage was switched on. Our analysis has revealed universal dependences of the loop area on the voltage frequency at low and high frequencies. The loop area approaches zero in both limiting cases, and its asymptotic behavior is given by

$$A(T)\sim\begin{cases}T^{-1}, & T\to\infty\\ T, & T\to 0.\end{cases} \tag{5.1}$$

For the voltage protocol in Eqs. (4.1) and (4.2), we can specify the relations in Eq. (5.1) and indicate the dependence on the voltage amplitude. Using the results in Eqs. (4.26), (4.27), (4.39), and (4.40), we can write

$$A(T) \sim \begin{cases} \dfrac{(\Delta V)^2}{T}, & \Delta V \to 0, \quad T \to \infty \\ T(\Delta V)^2, & \Delta V \to 0, \quad T \to 0 \\ \dfrac{\Delta V}{T}, & \Delta V \to \infty, \quad T \to \infty \\ Te^{\Delta V}, & \Delta V \to \infty, \quad T \to 0. \end{cases} \tag{5.2}$$

The frequency dependence of the loop area in the two limits has been discussed in many publications devoted to quite different physical problems in which hysteresis takes place.[16–27] It has been found that in the low-frequency regime ($T \to \infty$), the area approaches zero as $T^{-\beta}$ with $\beta \leqslant 1$. The area also vanishes as $T \to 0$. Its asymptotic behavior in this high-frequency regime is given by $A \sim T$. Thus, the two-state model of the ion channel leads to typical asymptotic behavior of the hysteresis loop area in both limits with $\beta = 1$ in the low-frequency regime.

Our analysis is based on the two-state Markovian model of channel gating,[8–11] Eq. (2.2), with the time-dependent transition rates controlled by periodic external voltage. Such a description arises as a special limiting case corresponding to the semiadiabatic approximation[28] of the more general stochastic dynamics in a double-well potential perturbed by a periodic external force. Semiadiabatic approximation is applicable when the characteristic intrawell relaxation times are much shorter than both the period of the external voltage and the characteristic interwell equilibration time. One can find a detailed discussion of this and related questions by Talkner and Luczka in Ref. 29. We believe that semiadiabatic approximation is highly appropriate to describe the effect of perturbation of the conformational equilibria of channel-forming proteins by periodic external voltages.

ACKNOWLEDGMENTS

This study was supported by the Intramural Research Program of the NIH, Center for Information Technology, and National Institute of Child Health and Human Development. One of the authors (M.A.P.) also thanks the Russian Foundation for Basic Research (Project No. 05-02-17626), the Scientific Council "Superconductivity," and the State programs "Quantum Macrophysics" and "Strong correlated electrons in semiconductors, metals, superconductors and magnetic materials" for partial support.

[1] B. Hille, *Ion Channels in Excitable Membranes* (Sinauer Associates, Sunderland, MA, 2001).
[2] W. Zhou, F. S. Cayabyab, P. S. Pennefather, L. C. Schlichter, and T. E. DeCoursey, J. Gen. Physiol. **111**, 781 (1998).
[3] A. Mathes and H. Engelhardt, J. Membr. Biol. **165**, 11 (1998).
[4] M. C. Menconi, M. Pellegrini, M. Pellegrino, and D. Petracchi, Eur. Biophys. J. **27**, 299 (1998).
[5] L. Kaestner, P. Christophersen, I. Bernhardt, and P. Bennekou, Bioelectrochemistry **52**, 117 (2000).
[6] R. Männikkö, S. Pandey, H. P. Larsson, and F. Elinder, J. Gen. Physiol. **125**, 305 (2005).
[7] J. Juraszek, B. Dybiec, and E. Gudowska-Nowak, Fluct. Noise Lett. **5**, L259 (2005).
[8] P. Mueller and D. O. Rudin, J. Theor. Biol. **4**, 268 (1963).
[9] G. Ehrenstein, H. Lecar, and R. Nossal, J. Gen. Physiol. **55**, 119 (1970).
[10] D. Sigg, H. Qian, and F. Bezanilla, Biophys. J. **76**, 782 (1999).
[11] F. Bezanilla, Physiol. Rev. **80**, 555 (2000).
[12] O. Flomenbom, J. Klafter, and A. Szabo, Biophys. J. **88**, 3780 (2005).
[13] W. J. Bruno, J. Yang, and J. E. Pearson, Proc. Natl. Acad. Sci. U.S.A. **102**, 6326 (2005).
[14] A. Fulinski, Z. Grzywna, I. Mellor, Z. Siwy, and P. N. R. Usherwood, Phys. Rev. E **58**, 919 (1998).
[15] S. Mercik, K. Weron, and Z. Siwy, Phys. Rev. E **60**, 7343 (1999).
[16] P. Jung, G. Gray, R. Roy, and P. Mandel, Phys. Rev. Lett. **65**, 1873 (1990).
[17] W. S. Lo and R. A. Pelcovits, Phys. Rev. A **42**, 7471 (1990).
[18] M. Rao, H. R. Krishnamurthy, and R. Pandit, Phys. Rev. B **42**, 856 (1990).
[19] A. Hohl, H. J. C. van der Linden, R. Roy, G. Goldsztein, F. Broner, and S. H. Strogatz, Phys. Rev. Lett. **74**, 2220 (1995).
[20] G. Goldsztein, F. Broner, and S. Strogatz, SIAM J. Appl. Math. **57**, 1163 (1997).
[21] D. Bose and S. K. Sarkar, Phys. Rev. E **56**, 6581 (1997).
[22] N. Berglund and H. Kunz, J. Phys. A **32**, 15 (1999).
[23] J. C. Phillips and K. Schulten, Phys. Rev. E **52**, 2473 (1995).
[24] M. C. Mahato and S. R. Shenoy, Phys. Rev. E **50**, 2503 (1994).
[25] M. C. Mahato and A. M. Jayannavar, Physica A **248**, 138 (1998).
[26] B. K. Chakrabarti and M. Acharyya, Rev. Mod. Phys. **71**, 847 (1999).
[27] H. Zhu, S. Dong, and J.-M. Liu, Phys. Rev. B **70**, 132403 (2004).
[28] P. Talkner, New J. Phys. **1**, 4 (1999).
[29] P. Talkner and J. Luczka, Phys. Rev. E **69**, 046109 (2004).